

Impulse stress waves emerged by laser target impulse coupling

ターゲットとレーザーのインパルス結合によって創発されるインパルス応力波の研究

Yoshiaki Tokunaga, Motoaki Nishiwaki[†], Mieko Kogi and Koji Aizawa (Kanazawa Institute of Technology.)

得永 嘉昭, 西脇 基晃[†], 小木 美恵子, 會澤康治 (金沢工大)

1. Introduction

As an attractive method for foreign gene transfection or drug delivery into cell, method of laser induced stress wave has been focused remarkably [1-3]. It has advantages in several characteristics of nonchemical, nonviral and noninvasive one. However, it has not been researched the accumulation of basic knowledge in detail. In order to develop reformed technique for delivering drugs or genes with high efficiency and safety into cell membranes, detail analytical investigation in a series of phenomena from ablation and plasma to shock wave should be reviewed again in a basic foundation. In this paper, we intend to discuss physical aspects of stress waves by pulsed laser-target impulse coupling in the case of direct geometry.

2. Laser induced stress wave (LISW)

Ultrasonic wave we pay attention is positive going wave (compression wave only) created in C-H material target. We call it "laser induced stress wave (LISW)". What is the LISW? It is formed due to complex phenomena such as thermoelastic, ablation, plasma and shock wave in distinguishing with ordinary stress wave defined in ultrasonic or sonic regime. In particular, analytical discussion in confined geometry for intensity enhancement of the LISW used by many investigators is very difficult. So as a first step, we will discuss physical aspect in direct geometry. **Figure 1** shows schematic diagram for explanation of these phenomena induced on or near the surface of the target made by C-H materials when the irradiated intensity of the pulse laser was increased continuously from ablation threshold to the above plasma threshold.

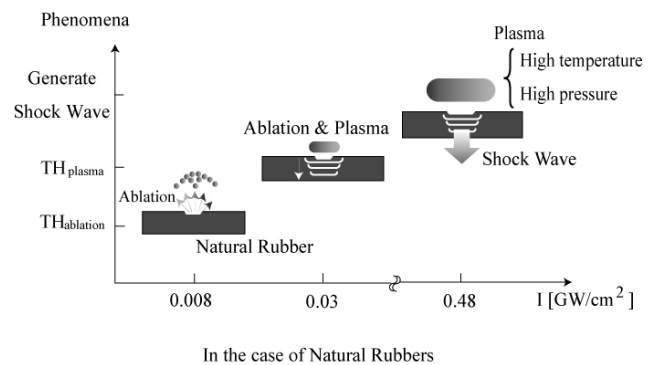


Fig. 1 Stress wave and I[GW/cm²]

Analytically, these phenomena were constituted from three steps. In first step, intensity below ablation threshold $TH_{ablation}$, generation and dynamic of laser induced stress wave correspond to thermoelastic wave [4]. This wave is composed of both positive and negative components. In second step, laser ablation begins to occur when irradiated intensity increases above $TH_{ablation}$. In this situation, ablation materials such as ion particles and electrons from surface of the target irradiated may be ejected in atmosphere of air. In additional increase of laser intensity, plasma will be formed near the surface when intensity becomes exceed of plasma threshold TH_{plasma} . In this final state, apparent wave shifts to positive wave. In final stage, shock wave may be formed in critical region near the surface. In this case it propagates with supersonic speed, exceeding Mach speed, toward other surface of the target as impulse pressure wave having additional recoil momentum by shock wave due to plasma with high temperature and pressure. In this field, stress wave, of course, has ns rise-time, ns FWHM, and GW/cm² order laser intensity.

E-mail address: toklab@mlist.kanazawa-it.ac.jp

On the basis of above explanation, we describe important factors as follows:

(2.1) Heating layer thickness (Fig. 2(b))

Heated layer in endothermic surface absorbing planar targets of C-H materials can be evaluated by equation (1) [5]

$$X_{th} = 0.97\sqrt{\alpha_{thermal}\tau} \quad (1)$$

In equation (1), X_{th} is the heated layer thickness at the end of the irradiation pulse. Since our laser impulse duration (full width half maximum: FWHM) is fixed at about 15 ns, X_{th} can be determined by thermal diffusivity $\alpha_{thermal}$ of target. In our experiment $\alpha_{thermal}$ of a natural rubber used was about $1.35 \times 10^{-7} \text{ m}^2/\text{s}$ and also X_{th} was about 35 nm

(2.2) Ablation pressure P_a (Fig. 2(c))

Important three parameters for estimation of P_a [kbars] are, respectively, intensity I GW/cm^2 , irradiation wavelength λ μm and FWHM τ ns (see Fig. 2(a)). We know that opto-mechanical coefficient C_m can be determined by product $I\lambda\sqrt{\tau}$ in ranging from 2 to 7 orders from Los Alamos experiments [4]. According to explanation of R.Fabbro et al [6], pressure P_a above ablation threshold in practical units obtained in the ranging from $I=0.1$ to $10^3 \text{ GW}/\text{cm}^2$ can be estimated by equation (2).

$$P_a = 3.93I^{0.7} [\text{GW}/\text{cm}^2] \times \lambda^{-0.3} [\mu\text{m}] \times \tau^{-0.15} [\text{ns}] \quad (2)$$

(2.3) PVDF transducer detection (Fig.2(c))

A PVDF film transducer can be usually used to estimate P_a on surface of C-H material target. However, detected signal is transformed as voltage value V_{pvdf} corresponding with P_a . So we attempt to evaluate P_a from measured V_{pvdf} . Figure 3 shows relationship with P_a simulated by using eq. (2) and measured V_{pvdf} when I is increased continuously from 0.08 to 0.50 GW/cm^2 .

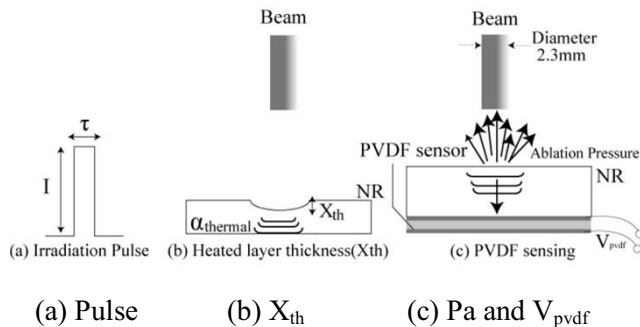


Fig. 2 Explanation of X_{th} , P_a and $V_{pvd f}$

P_a is approximately proportional to those of measured V_{pvdf} in ranging from 0.1 to 0.35 GW/cm^2 . From experimental and simulated results, we can use a simple equation as shown in eq.(3).

$$P_a [\text{kbars}] = K^n V_{PVDF} [V] \quad (3)$$

In equation (3), K is arbitrarily constant, and n is integer, respectively. In our experimental condition K and n were 0.6 kbars /V and 1.0, respectively. In this way, we can estimate approximately that P_a corresponded with about 1.75 kbars when measured PVDF transducer voltage was about 3 V. However we found that discrepancy between P_a and V_{pvdf} at above $I = 0.35 \text{ GW}/\text{cm}^2$ in Fig. 3 could not be ignored.

3. Conclusion

We showed physical description due to several equations on pulse laser-target impulse coupling in direct geometry (air target boundary) and ablation pressure on target's surface could be approximately estimated from detection voltage of PVDF film transducer.

Acknowledgement

This work was partly supported by a Grant-in-Aid for challenging Exploratory Research (No.23656275) from the Japan Society for the Promotion of Science (JSPS).

References

1. A.G.Doukas et al: Ultra.Med.& Biol.,1 (1993)137
2. M.Terakawa et al: Jpn. J. Appl. Phys., 46 (2007),1243
3. M.Kogi et al: IEICE Tech. Rep., US2010-97 (2011) 31
4. F.W.Cross et al: Appl. Phys. Lett., 50 (25) (1987) 1019
5. C.R.Phipps et al: J. Appl. Phys, 64 (3) (1988) 1083
6. R.Fabbro et al: J. Appl. Phys, 68 (2) (1990) 775

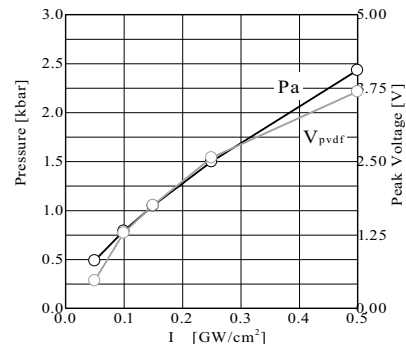


Fig. 3 Comparison with P_a and $V_{pvd f}$